LIDAR AND RADAR INVESTIGATION OF INERTIA GRAVITY WAVE INTRINSIC PROPERTIES AT MCMURDO, ANTARCTICA

Cao Chen [1], Xinzhao Chu[1], Zhibin Yu[1], Weichun Fong[1], Adrian J. McDonald[2], Xian Lu[1], and Wentao Huang[1]

[1]*University of Colorado at Boulder, 216 UCB, CIRES, Boulder, CO 80309, USA, Email: Cao.Chen@Colorado.edu*
[2]*University of Canterbury, Department of Physics and Astronomy, Christchurch, NZ*

ABSTRACT

A new lidar campaign ongoing at McMurdo (77.8° S, 166.7° E), Antarctica has provided high-resolution temperature data in the mesopause region, which are used to extract the dominant gravity waves. On 11 July 2011, a coherent inertia gravity wave (IGW) structure was observed in both Fe lidar temperature and MF radar wind. The observed wave period is ~7.15 h and the vertical wavelength is ~20 km. With simultaneous measurements of temperature and wind, the intrinsic wave properties were determined using a temporal hodograph method. The results show that the intrinsic period of the wave is 7.47 h, and the wave is propagating toward the azimuth direction of 62° clockwise from the north with a large horizontal wavelength of ~1975 km. The horizontal intrinsic phase speed is 73.4 m/s. The horizontal group velocity is ~39 m/s and the vertical group velocity is 0.44 m/s. The positive intrinsic period indicates the upward propagation of wave energy but with a very small propagation angle (~0.6°) from the horizon. The IGW may have originated from a geostrophic adjustment of the jet stream on the opposite side of the Antarctic continent.

1. INTRODUCTION

Gravity waves have been recognized to be important because of their major impacts in driving the mean meridional circulations, affecting thermal structure and constituent transport. Long-duration, large-altitude-range and high-resolution measurements of gravity waves are essential to provide constraints for gravity wave parameterizations. The long-standing "cold pole" problem in many models can be attributed in large part to underestimated wave drag induced by IGWs or short period waves. IGWs are long-period waves that are influenced by the rotation of the Earth. They are often observed in the troposphere and stratosphere [1]. It has been demonstrated that the horizontal wavelengths of IGWs can be thousands of kilometers, while the vertical group velocity just a few centimeters per second. In the mesosphere and lower thermosphere (MLT) region, there have been observations of IGWs using lidars [2, 3] and incoherent scatter radar [4]. Similarly, large horizontal wavelengths were retrieved in these studies. Investigations of IGW in the mesopause region over Antarctica are rare yet important due to its potential influence on MLT temperatures and dynamics [4].

The University of Colorado lidar group deployed an Fe Boltzmann lidar to McMurdo since Dec 2010 [5]. This lidar has full diurnal coverage and is capable of measuring temperatures at altitudes between 30 and 110 km [6]. The Scott Base MF radar is co-located with the Fe lidar at Arrival Heights. This radar has near-continuous temporal coverage and has been collecting MLT wind data at heights between 70 and 100 km since 1982 [7]. The simultaneous MLT temperature and wind data provide a unique opportunity for studying the IGWs and their intrinsic properties at this high southern latitude.

2. DATA ANALYSIS

2.1 Derivation of Wave Perturbations

As shown in a companion paper [6], the temperatures in the McMurdo MLT observed by the lidar show strong wave activity. In particular, wave oscillations with periods of 5–8 h dominate the temperature variations, especially in the winter months. These dominant waves are likely inertia gravity waves.

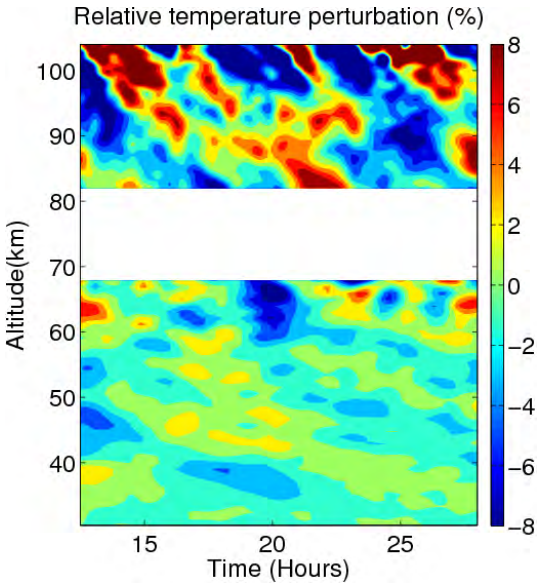

Figure 1. Relative temperature perturbations after removing tides and high-frequency perturbations on 11 July 2011.

The MLT temperature data we used have resolutions of 0.1 h and 0.1 km, and MF radar data have resolutions of 0.5 h and 2 km. The Fe lidar data were smoothed

temporally and vertically with Hamming windows of 0.5 h and 1 km FWHM. Therefore, only the waves with periods longer than 1 h, and vertical wavelength longer than 2 km were resolved.

Relative temperature perturbations were derived by subtracting the mean temperature at each altitude and then divided by the mean. In order to minimize the contamination of tidal oscillations in the temperature perturbations, a linear trend in the time domain at each altitude is removed, followed by a subtraction of a linear trend in the spatial domain at each moment [2]. Figure 1 shows the relative temperature perturbations from 35 to 105 km on 11 July 2011. A clear downward phase progression shows a vertical wavelength of 20 km around MLT region. To derive the gravity-wave-induced wind perturbations from MF radar data, the tidal effect was removed by subtracting a temporal fitting of diurnal and semi-diurnal–period sinusoidal functions at each altitude from the original wind observations.

2.2 Hodograph Method

Hodograph methods have been used to study gravity wave intrinsic properties in MLT regions by many analyses using wind and temperature data, such as in [2]. Most of the studies apply hodograph analysis over height. However, for this study, we chose temporal hodograph instead for the following two main reasons. Firstly, the radar wind measurements only have a 2 km vertical resolution, so that there are usually not enough sequential height data to obtain a significant result, especially when the vertical wavelength is short. Secondly, the overlapping observation range between lidar and MF radar is usually confined to 20 km (from 80 to 100 km), which is not long enough to accurately resolve gravity waves with longer vertical wavelengths (≥20 km). The lidar measurements in the last 15 months have revealed that gravity waves with such wavelengths are common at McMurdo. Therefore, the subsequent analysis will be restricted to temporal hodograph.

In-phase wind perturbation and quadrature-phase wind perturbation amplitude are related by the equation below,

$$\tilde{U} = i\frac{\hat{\omega}}{f}\tilde{V}, \tag{1}$$

where $\tilde{U}$ is the in-phase wind perturbation, $\tilde{V}$ is the quadrature-phase wind perturbation, $\hat{\omega}$ is intrinsic frequency of the wave, and f is Coriolis parameter, corresponding to a 12.24-h inertial period at McMurdo (77.8° S). Eq. (1) shows that gravity-wave-induced in-phase and quadrature-phase wind perturbations ($\tilde{U}, \tilde{V}$) exhibit elliptical polarization. In the Southern Hemisphere where f < 0, $\tilde{U}$ will lead $\tilde{V}$ and ($\tilde{U}, \tilde{V}$) will rotate counterclockwise with time if the wave propagates upward ($\hat{\omega} > 0$). The relation between temperature perturbation and the in-phase wind perturbation amplitudes is given by Eq. (2):

$$\tilde{T} = \frac{1}{g}\left(im + \frac{1}{2H}\right)\frac{\hat{\omega}^2 - f^2}{\hat{\omega}k_h}\tilde{U}, \tag{2}$$

where m is the vertical wave number, k_h is the horizontal wave number, H is scale height, and $\tilde{T}$ is the relative temperature perturbation. Eq. (2) shows that there is a fixed phase relationship between $\tilde{T}$ and $\tilde{U}$. Specifically, fit relative temperature perturbation and in-phase wind perturbation to the quasi-monochromatic gravity wave model given below,

$$U' = \left|\tilde{U}\right|\cos(\omega t + \Phi_U), \tag{3}$$

$$T' = \left|\tilde{T}\right|\cos(\omega t + \Phi_T). \tag{4}$$

The phase information deduced from the fitting will exhibit a relation as follows.

$$\Phi_U - \Phi_T = \tan^{-1}(m \cdot 2H). \tag{5}$$

Consequently, Eq. (5) can be used to determine the wave propagation direction in the horizontal plane.

The intrinsic frequency $\hat{\omega}$ can be calculated from the amplitude ratio between $\tilde{U}$ and $\tilde{V}$ derived from the hodograph using Eq. (1). However, our investigation shows that the amplitude ratio of the fitted ellipse varies dramatically with altitude but the major axis remains in similar directions. Therefore, we take a different approach that utilizes the major axis direction of the ellipse fitting, instead of amplitudes, to estimate intrinsic frequency. From the dispersion relationship, definition of intrinsic frequency, and by assuming small background wind shear [8], we have,

$$\begin{cases} {k_h}^2 = \dfrac{\hat{\omega}^2 - f^2}{N^2 - \hat{\omega}^2}\left(m^2 + \dfrac{1}{4H^2} - \dfrac{\hat{\omega}^2}{{c_s}^2}\right), & (6) \\ \hat{\omega} = \omega - k_h\bar{U}, & (7) \end{cases}$$

Thus, $\hat{\omega}$ can be solved from the following equation:

$$\left(\frac{1}{c_s^2} - \frac{1}{\bar{U}^2}\right)\hat{\omega}^4 + \frac{2\omega}{\bar{U}^2}\hat{\omega}^3 + \left(\frac{N^2 - \omega^2}{\bar{U}^2} - m^2 - \frac{1}{4H^2} - \frac{f^2}{c_s^2}\right)\hat{\omega}^2 - \frac{2N^2\omega}{\bar{U}^2}\hat{\omega} + f^2\left(m^2 + \frac{1}{4H^2}\right) + \frac{N^2\omega^2}{\bar{U}^2} = 0. \tag{8}$$

where c_s is speed of sound, $\bar{U}$ is the horizontal mean wind projected onto the wave propagation direction, N is the buoyancy frequency. Eq. (8) has four roots, but only the meaningful solution will be selected. Details will be discussed in the next section.

3. RESULTS AND DISCUSSION

On 11 July 2011, a coherent wave structure was observed in both lidar temperature and radar wind from 81 to 89 km as shown in Figure 2, suggesting that these two instruments observed the same gravity wave event. Therefore, temporal hodograph analysis was used to derive the intrinsic parameters.

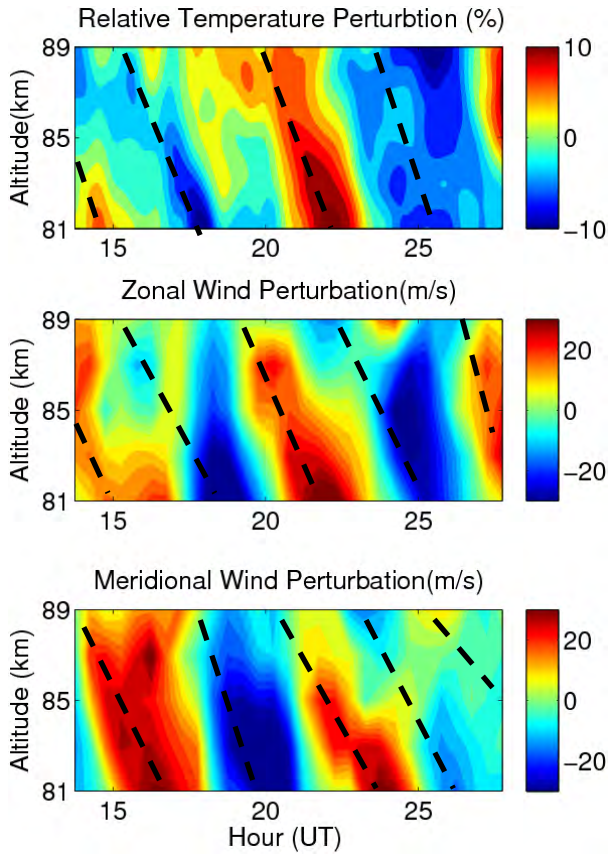

Figure 2. From top to bottom, relative temperature, zonal wind, and meridional wind perturbations on 11 July 2011 at McMurdo, after tides and high-frequency waves are removed.

The procedure was to first determine the dominant observed period T_O from the Lomb-Scargle spectrum analysis of the temperature, zonal wind, and meridional wind at each altitude. Then, all three datasets were band-pass filtered around the dominant observed frequency ω with cutoff periods at 10 and 5 h.

The band-pass filtered wind perturbations were then plotted on a hodograph (see Figure 3). As shown in Figure 3, all three ellipses at three altitudes are elongated in nearly northeast direction. The least mean square (LMS) fitting of all three ellipses showed that the azimuth angle was 62° or 62°+180°=242°. (The direction is defined to be 0°at north and increase clockwise). The 180° ambiguity was resolved by making use of Eq. (5). In doing so, we first chose the wave propagation direction as the bearing of the red arrow in Figure 3. Zonal and meridional wind perturbations were then projected to the new x-axis to obtain the in-phase wind perturbations. Both in-phase wind perturbations and relative temperature perturbations were fitted to model (3) and (4). The deduced phase difference between Φ_U and Φ_T is very close to the one calculated from Eq. (5), with a discrepancy of ~π/5, which indicates that the wave was propagating in the direction as shown by the red arrow in Figure 3, i.e., 62° east of north. The in-phase background wind ($\bar{U}$) was then derived by projecting horizontal wind onto the propagation direction and fitting a mean value plus a sinusoidal wave. The period of the sinusoidal wave is set equal to the period of the observed gravity wave. In this case, the projected mean wind was calculated to be 3.3±1 m/s by averaging the values in the altitude range.

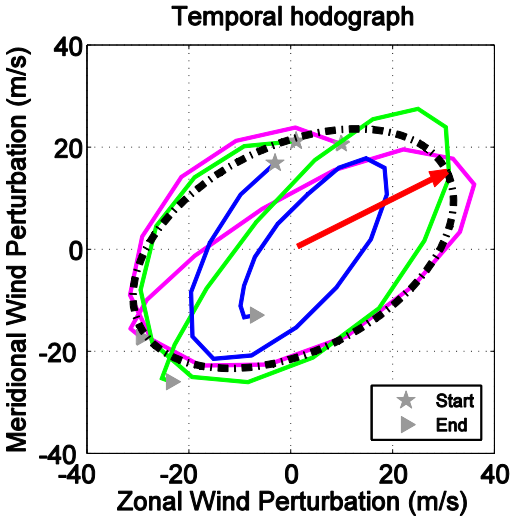

Figure 3. Hodographs of zonal and meridional wind perturbations on 11 July 2011. Three hodographs (at 81, 83 and 85 km) are plotted together, where stars and triangles denote the beginning and end of the data.

Finally, the intrinsic frequency ($\hat{\omega}$) was solved from Eq. (8). The calculated intrinsic periods are 7.47, 6.81, -0.09, and 0.09 h, corresponding solutions for horizontal wavelength are 1975, -1728, -1.1, and 1.08 km, respectively. The last two solutions are unreasonable because the wavelengths are too small considering the MF radar field of view is ~30°. Since the propagation direction of the wave has been determined, only the positive wavelengths would be acceptable. Therefore, the first pair of solutions was selected so that intrinsic period of the wave is 7.47 h and the horizontal wavelength is 1975 km. The apparent horizontal phase speed is 76.7 m/s, while the intrinsic horizontal phase speed is 73.4 m/s. The group velocity was also calculated using Eqs. (9–10),

$$c_{gh} = \frac{k_h(N^2 - \hat{\omega}^2)}{\hat{\omega}\left({k_h}^2 + m^2 + \frac{1}{4H^2}\right)}, \qquad (9)$$

$$c_{gz} = -\frac{m(\hat{\omega}^2 - f^2)}{\hat{\omega}\left({k_h}^2 + m^2 + \frac{1}{4H^2}\right)}, \quad (10)$$

Horizontal group velocity was found to be ~39 m/s, while the vertical group velocity was 0.44 m/s, i.e., 38 km/day in the vertical direction. The elevation angle of the energy propagation was ~0.6° from the horizon, which indicates that the wave source might be very far from the McMurdo station as discussed below.

The group velocities we calculated above indicate that the vertical group velocity was significantly slower than the horizontal group velocity. This implies that it would take ~1–2 days for the wave to propagate a vertical distance of ~40–80 km, if the vertical wind is negligible. During this period, the wave would have propagated ~5500 km in the horizontal plane, if we assume the background wind along the wave propagation path was negligible (although this may not be true). Certainly, if the background winds at lower altitudes were against the wave propagation direction, the horizontal distance and time needed to reach mesopause would be shorter [4].

The wave propagation direction derived from the hodograph is toward ~62° clockwise from the north. If we assume the wave propagating along this direction with nearly constant group velocity during the 1–2 days of period, the large horizontal propagation range would place the wave source on the opposite side of the Antarctic continent around 50–40°S and 55°E. This is close to the jet stream locations. As Nicolls et al. [4] argued in analyzing the IGWs observed in the Arctic, a possible mechanism of generating IGWs is a geostrophic adjustment of the jet stream. Although the exact source location could not be pinpointed, Vadas' wave modeling demonstrated such a generation mechanism. Similarly, we speculate the IGW observed at McMurdo could be excited by a geostrophic adjustment of the jet stream on the opposite side of the Antarctic continent, located 5000–6000 km away from McMurdo. The wave may have propagated for 1-2 days prior to our observations.

4. CONCLUSIONS AND OUTLOOK

The hodograph analysis has been applied to the combined Fe lidar/ MF radar data of temperature and wind. A dominant inertia-gravity wave has been observed. This is the first time that a coincident observation of an inertia-gravity wave by an MF radar and lidar is reported in Antarctica. Our further analysis has also indicated another IGW event with an intrinsic period of 7.5 h on 29 June 2011. This suggests that there could be active wave sources generating these large-scale inertia-waves during winter. Although IGWs were thought to be of secondary importance to the MLT region, our lidar measurements indicate that the IGWs have significant impacts on the MLT temperature at McMurdo. Therefore, it is crucial to evaluate the roles of IGWs in the polar region.

Whether the geostrophic adjustment of the jet stream is responsible for the observed IGWs deserves further investigations with wave modeling and ray-tracing test. Background wind information is crucial in tracing the waves to their source regions. Our temporal hodograph method also needs validation against other approaches and assessment of the possible influence by the background wind shear.

ACKNOWLEDGEMENTS

We acknowledge Zhangjun Wang, John A. Smith and Brendan Roberts for their contributions to the McMurdo lidar campaign. We appreciate the staff of McMurdo and Scott Base for their superb support. The lidar project was supported by the USA National Science Foundation OPP grant ANT-0839091. AJM thanks Antarctica New Zealand for the logistic support for the MF radar.

REFERENCES

1. Sato, K., D. J. O'Sullivan, T. J. Dunkerton, 1997: Low-frequency inertia-gravity waves in the stratosphere revealed by three-week continuous observation with the MU radar, *Geophys. Res. Lett.,* **24**, 1739-1742.

2. Lu, X., A. Z. Liu, G. R. Swenson, T. Li, T. Leblanc, I. S. McDermid, 2009: Gravity wave propagation and dissipation from the stratosphere to the lower thermosphere*, J. Geophys. Res.,* **114**, D11101

3. Li, T., et al., 2007: Sodium lidar – observed strong inertia-gravity wave activities in the mesopause region over Fort Collins, Colorado (41°N, 105°W), *J. Geophys. Res.,* **112**, D22104.

4. Nicolls, M. J., R. H. Varney, S. L. Vadas, P. A. Stamus, C. J. Heinselman, R. B. Cosgrove, M. C. Kelley, 2010: Influence of an inertia-gravity wave on mesospheric dynamics: A case study with the Poker Flat Incoherent Scatter Radar*, J. Geophys. Res.,* **115**, D00N02.

5. Chu, X., et al., 2011: First lidar observations of polar mesospheric clouds and Fe temperatures at McMurdo (77.8°S, 166.7°E), Antarctica, *Geophys. Res. Lett.,* **38**, L16810.

6. Chu, X., Z. Yu, C. Chen, et al., 2012: McMurdo lidar campaign: A new look into polar upper atmosphere, Proc. 26th ILRC, Greece.

7. Baumgaertner, A. J. G., A. J. McDonald, G. J. Fraser, G. E. Plank, 2005: Long-term observations of mean winds and tides in the upper mesosphere and lower thermosphere above Scott Base, Antarctica, *J. Atmos. Sol.-Terr. Phys*., **67**, 1480-1496.

8. Fritts, D. C., and M. J. Alexander, 2003: Gravity wave dynamics and effects in the middle atmosphere, *Rev. Geophys.*, **41(1)**, 1003.